Experimental Study of the Ferroelastic Phase Transition in Urea/*n*-Heptadecane Composite

T. Breczewski,*,† A. López-Echarri,‡ L. Rubio-Peña,† M. I. Aroyo,‡ I. Ruiz-Larrea,*,† and E. H. Bocanegra†

Departamento de Física Aplicada II, Departamento de Física de la Materia Condensada, Facultad de Ciencia y Tecnología, Universidad del País Vasco, Apartado 644, 48080 Bilbao, Spain

Received: October 30, 2006; In Final Form: February 5, 2007

An experimental study of the ferroelastic phase transition in urea/*n*-heptadecane $CO(NH_2)_2/C_{17}H_{40}$ composite around the structural phase transition undergone by this crystal at 159 K is presented. The temperature dependence of the macroscopic spontaneous strain and the optical birefringence around this temperature has been determined. A phenomenological model limited to the hexagonal−orthorhombic change of the urea sublattice leads to a linear relation between these quantities and the phase transition entropy. The experimental data agree with this description exception made of the near vicinity of the phase transition, where the influence of the alkane chain ordering processes cannot be excluded.

1. Introduction

Urea inclusion compounds are prototype examples of organic supramolecular materials. This type of composite materials is of particular interest because of the structural and dynamical properties together with the interactions between the involved self-organized molecules. The knowledge of these interactions may permit to understand the mechanism of the ferroelastic phase transitions that appeared in these materials in the low-temperature region.

The crystals of urea/*n*-alkane (we will use the notation C*n*; *n* = number of carbons of the alkyl chain) belong to the family of crystals with molecular incommensurate composite structures.[1] As first reported by Schlenk and Zimmerschield[1] (and references therein), the urea molecules are connected by hydrogen bonds to form helical ribbons with six molecules per helical pitch (11 Å). They define an array of linear, hexagonal nanoporous tunnels (host structure) where the guest molecules are packed end-to-end. The channel centers of this honeycomb network are separated by approximately 8.2 Å. The diameter of the tunnels (approximately 5.5 Å) together with the helical pitch strongly restricts the type of guest molecules that can be accommodated inside them.[2,3] Therefore, only long-chain hydrocarbons or substituted hydrocarbon molecules are permitted for stable urea inclusion compounds.

For such crystals, the structural periodicity is defined by three parameters: c_g, which corresponds to the guest molecules repeat distance along the channel axis and, c_h, which corresponds to the urea (host) sublattice periodicity in the same direction. The c_h and c_g ratio (the so-called misfit parameter) is usually incommensurate in urea inclusion compounds.[4] The third parameter is Δ_g, which represents the offset between the positions of the molecules in any pair of adjacent tunnels. In particular, if the guests are alkane groups, $\Delta_g = 0$.[5]

In the case of many alkane guests, the mean room-temperature structure of the host subsystem is described by the hexagonal $P6_122$ space group.[2,6,7] In this phase, the urea subsystem is formed by hydrogen bonds and is influenced by the symmetry of the confined guest alkane molecules chains which are usually planar. These alkane molecules occupy a 6-fold axis position in the urea channels and are characterized by rotational disorder at room temperature.

At decreasing temperature, the urea sublattice exhibits a phase transition to an orthorhombic phase $P2_12_12_1$.[8] Up to now, the superspace group of the low-temperature phase is not yet established and a structural refinement of this phase has not been reported. Both attempts have to cope with the difficulties arising from the large number of domains generated at the phase transition. In the case of the *n*-alkane guest, the orthorhombic low-temperature phase contains a number of broken-symmetry induced domains that do not fit with the quotient between the para- and ferroelastic point group orders.[9] As these domains are ferroelastic, X-ray and neutron diffraction present complex patterns that prevent structural refinements.

A fundamental problem concerns the molecular interactions and the kind of mechanism triggering the phase transition in these crystals. One of the possible mechanisms is related with the shearing of the structure of urea in the commensurate *a*,*b*-plane of the urea−host sublattice (normal to 6-fold axis of the room-temperature structure), which provokes a herringbone-like arrangement of the alkane-guest sublattice in the urea channels. The rotational motion around the alkane long axis is frozen in, and the molecular planes are oriented between opposite corners of the urea hexagonal channels, as shown by NMR measurements in C19.[10] As a consequence, the theoretical description of this phase transition, suggested by Lynden-Bell,[11] considers a coupling effect between an order−disorder (the alkane−guest sublattice) and a displacive (the urea−host sublattice) as the main mechanism of the phase transition.

The structure of C17 is almost commensurate in the direction parallel to the *c*-axis. Therefore, longer-range ordered structures parallel to *c*-axis may be favored.[8] From the temperature dependence of the diffuse layers profile, presented in the X-ray diffraction patterns of these crystals, the same authors conclude that the longitudinal correlations of the alkanes remain quite unaffected both by the lateral deformation of the host structure and by the freezing of the rotational degree of freedom of the

* E-mail: tomasz.breczewski@ehu.es (T.B.); isabel.ruiz@ehu.es (I.R.-L.).
† Departamento de Física Aplicada II.
‡ Departamento de Física de la Materia Condensada.

10.1021/jp067115v CCC: $37.00 © 2007 American Chemical Society
Published on Web 04/24/2007

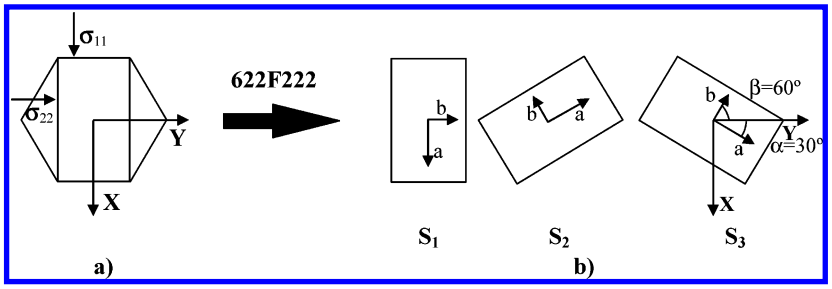

Figure 1. (a) The Cartesian frame used for the orientation of the crystal samples and the angle measurements. (b) Orientation states arising at 622F222 ferroelastic phase transition, according to the classical symmetry approach of Sapriel.

guest molecules around their long axis near the phase transition temperature T_c.[8]

The phase boundary between the hexagonal−orthorhombic phase was observed by optical studies of the ferroelastic domain structure around T_c.[12] The existence of the phase boundaries in the urea/*n*-heptadecane crystals C17, and its absence in C19, C20, and C22 compounds, suggests a particular feature of that phase transition.[13]

The studies presented in this paper are focused on the C17 phase transition. The specific heat measurements by adiabatic and AC calorimetry showed that the phase transition undergone by this crystal is characterized by a double peak anomaly centered about 158.9 K. The profile of the temperature dependence of the specific heat depends on the heating rate and on the thermal history, but these two peaks were always observed. This fact suggests that the phase transition in C17 takes place in two successive steps.[14] To confirm this behavior and to attain a deeper understanding of the physical mechanisms of this transformation, the temperature dependence of the macroscopic spontaneous strain and the birefringence were measured.[15] A phenomenological model that describes the main phase transition from the hexagonal to the orthorhombic phases of the urea sublattice was also developed. It results in a linear relation between the excess entropy and the spontaneous strain and the birefringence, which is compared with the experimental results.

2. Experimental Procedure and Results

2.1. Crystal Growth and Samples Preparation. Crystals of C17 were grown from a saturated solution of pure urea and the respective inclusion compound in a 50% methanol−propanol mixture by the isothermal dynamic method at 320 K. The obtained single crystals were of good optical quality, colorless and transparent. They show a prismatic hexagonal base with an edge length between 5 and 30 mm. To confirm the presence of the low-temperature phase transition, preliminary differential scanning calorimetric measurements from 100 to 300 K were performed. A Perkin-Elmer Pyris-1 DSC-model was used with a scanning rate of 10 K/min.

All samples are oriented, and all angle measurements are referred to a common Cartesian frame, fixed in the paraelastic phase (Figure 1a). The Cartesian *z*-axis is chosen along the 6-fold axis (urea channel). The *y*-axis is parallel to the crystallographic *b*-axis, which is common to the hexagonal (paraelastic) and orthorhombic (ferroelastic) phases.

2.2. Spontaneous Strain and Domain Switching Process. The measured values of the macroscopic spontaneous strain are strongly influenced by the ferroelastic domain structure of the crystal.[15] The spontaneous strain, using macroscopic methods, can be measured only for monodomain crystal samples. Therefore, a previous study of the switching process of the domain structure was required.

The crystal samples for optical observation of the domain structure were cut out as rectangular parallelepipeds $5 \times 5 \times 1$ mm^3 in size with edges parallel to the crystallographic axes of the hexagonal phase and polished surfaces perpendicular to the *c*-axis. The samples were heated and cooled using a THMS 600 (Linkam) stage, which was adapted to apply an uniaxial stress to the crystal sample. Temperature was controlled within ±0.1 K resolution. Optical observations were performed along the *c*-axis using a polarizing microscope (Axioplan 2-Carl Zeiss Jena) equipped with a digital camera (Polaroid DMC Digital Microscope Camera).

Ferroelastic domains of C17 are very small compared with those commonly observed in other ferroelastic crystals and show a complex distribution. The angles between the domain walls and the crystallographic axes cannot be explained using only the classical symmetry approach of Sapriel[16] (Figure 1b). According to this description for the 622F222 phase transition of the urea sublattice, the number of the different ferroelastic orientation states should be three with six permissible W-type[16] domain walls among them. In the case of C17, domains of the same orientation state but slightly rotated around the 6-fold axis are present.[12] This type of domain structure was confirmed by the X-ray measurements[13] and also by direct optical observations using a polarizing microscope.[12] When external mechanical compressive stress $\sigma_1 < 0$ or $\sigma_2 < 0$ (Figure 1a) is applied to the polydomain sample, the switching processes is triggered. In the following, the Voigt notation for all the tensor quantities will be used.

In the case when only $\sigma_1 < 0$ is applied, the switching process occurs in such a way that S_2 and S_3 domains disappeared and an increased volume for the S_1 domain is observed for higher σ_1 absolute values. Finally, for $\sigma_1 = -0.4$ MPa at $T = 135$ K, the switching process is finished, and all the crystal volume is in the S_1 state (Figure 2b). When $\sigma_2 < 0$ is applied, a monodomain state cannot be reached (Figure 2c). For uniaxial stresses $\sigma_2 < -0.4$ MPa, the S_1 state disappears, but the S_2 and S_3 states remain. Only domain walls between these states in the planes $X = 0$ and $Y = 0$ can be observed (Figure 2c).

In order to obtain the thermal dependence of the macroscopic spontaneous strain, the thermal expansion under the uniaxial compressive stress was measured by the thermomechanical analysis (TMA) method,[17] using a Perkin-Elmer DMA-7 model. For these measurements, cubic crystal samples of $2 \times 2 \times 2$ mm^3 with edges parallel to each of the crystallographic axes were cut. Taking into account the very small temperature difference between the successive steps of the phase transition, when it is observed in calorimetric experiments,[14] a continuous method for the macroscopic spontaneous strain measurements was used. For this purpose, a fixed heating rate of 0.3 K/min from 120 to 300 K was chosen. This method has permitted us to measure the crystal thickness when the sample is statically stressed in the same crystallographic direction. As cited above,

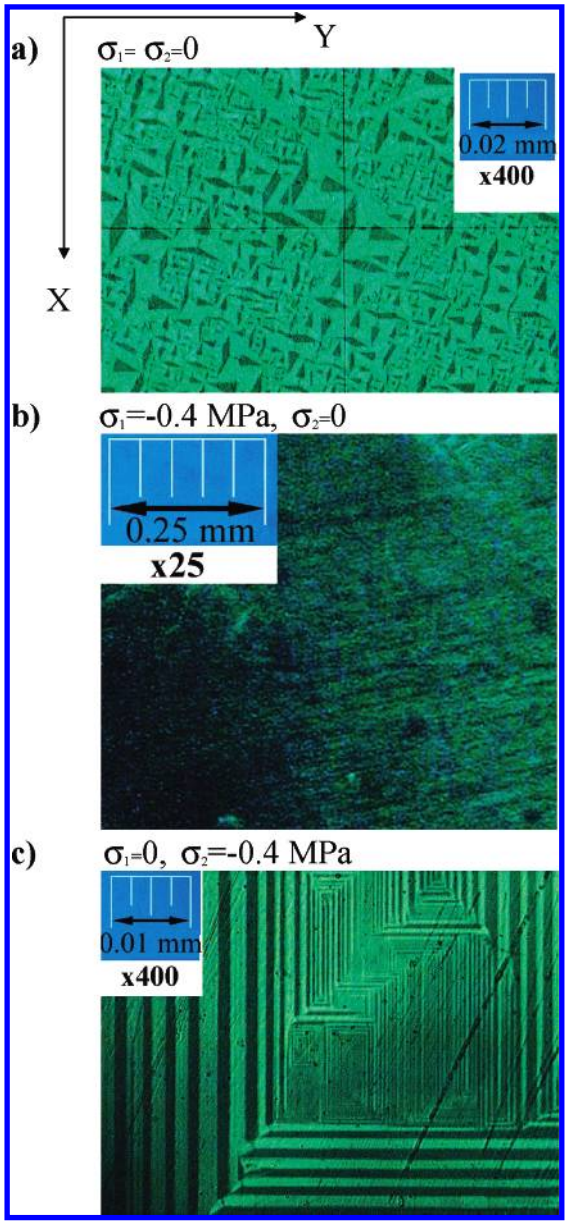

Figure 2. Switching process of the domain structure at $T = 135$ K. (a) The polydomain sample: $\sigma_1 = 0$ and $\sigma_2 = 0$. (b) The monodomain state: S_1 state, $\sigma_1 = -0$, 4 MPa and $\sigma_2 = 0$. (c) S_2 and S_3 states: $\sigma_1 = 0$ and $\sigma_2 = -0.4$ MPa.

in order to obtain a monodomain sample with S_1 orientation, a compressive static stress $\sigma_1 = -0.4$ MPa was applied (Figure 1a). Under these conditions, the temperature dependence of the sample thickness in the *X*-crystallographic direction, proportional to the cell constant value *a* in both the hexagonal and the orthorhombic phases, was determined. Using the standard compensation method for the thermal expansion,[15,18] we evaluated the strain tensor component ϵ_1 (Figure 3). When the static stress $\sigma_2 = -0.4$ MPa is applied, we assume an equal distribution for S_2 and S_3 orientation states, both occupying equal volume in the crystal. The measured deformation ϵ_y (Figure 3) can be expressed as a function of the strain components ϵ_1 and ϵ_2 of the orientation state S_1[19]

$$\epsilon_y = \epsilon_1 \cos^2 \alpha + \epsilon_2 \cos^2 \beta \qquad (1)$$

where the α and β angles are 30° and 60°, respectively (Figure 1b). The temperature dependences of ϵ_1 and ϵ_y permit us to

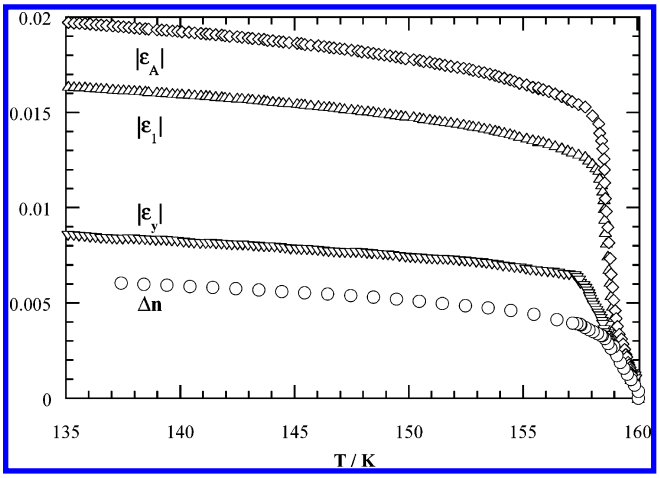

Figure 3. Thermal dependence of the non-dimensional quantities: the scalar spontaneous strain ϵ_A (◇), the strain components $\epsilon_1(\Delta)$ and ϵ_y (∇), and the birefringence Δn (○) performed on C17 crystal. Leaving apart Δn, only about 20% of the experimental points are represented.

calculate the values of the components of the spontaneous strain ϵ_i^S, which for the 622F222 ferroelastic species is given by

$$\epsilon_1^S = \frac{1}{2}(\epsilon_1 - \epsilon_2) \qquad \epsilon_2^S = -\frac{1}{2}(\epsilon_1 - \epsilon_2) \qquad (2)$$

where the remaining components are zero.

The scalar spontaneous strain ϵ_A defined by Aizu is[20]

$$\epsilon_A = \frac{\sqrt{2}}{2}(\epsilon_1 - \epsilon_2) \qquad (3)$$

In Figure 3, the temperature dependence of ϵ_A, ϵ_1, and ϵ_y is shown.

2.3. Birefringence. For the birefringence (Δn) measurements, the Ehringhaus tilting compensator was used. The calculation of the path difference was made for $\lambda = 551$ nm as a centroid of white light, whereas a sample constant thickness in all the temperature range is assumed. The optical observations were made continously along the crystallographic *c* direction in the temperature range 293−100 K. The birefringence was measured in the monodomain part of the crystal without external stress. These results are presented in Figure 3.

2.4. Calorimetric Measurements. Previous DSC heating and cooling runs from 170 to 300 K were performed. Varying rates from 2 to 10 °C/min permitted us to study the thermal hysteresis and to determine the total enthalpy associated with the phase transition.

The specific heat C_p of C17 was obtained by adiabatic calorimetry using the heating pulse and the dynamic thermogram methods[14] in the temperature range 80−330 K. The first procedure obtains the mean specific heat between two thermal equilibrium states, and the inaccuracy is limited to 0.1% of C_p. On the other hand, the density of the experimental points around the phase transitions can be significantly increased if thermograms with very low scanning rates (down to 0.1 °C/hour) are used. The ΔC_p excess associated to the phase transition was determined by subtraction of the so-called normal lattice specific heat. This contribution was determined by a simple extrapolation of the C_p values at both sides of the transition region. As it is limited to 25 °C around the peak, this direct procedure does not result in noticeable errors in ΔC_p. This quantity is shown in Figure 4, where only points obtained by the pulse method are plotted. The entropy excess ΔS is determined by means of

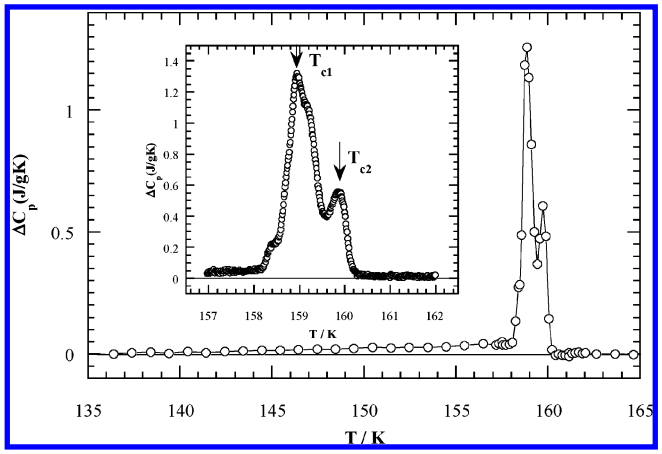

Figure 4. The specific heat excess ΔC_p associated to the phase transition of C17 measured by the pulse technique. The inset shows a calorimetric curve obtained by means of a heating thermogram at a rate of 0.6 °C/h.

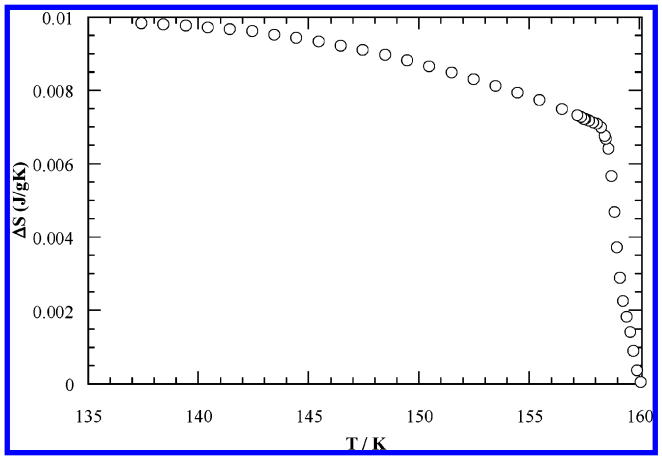

Figure 5. C17 entropy excess (ΔS) as a result of the integration of ΔC_p data.

a numerical integration of the experimental specific heat data using the expression

$$\Delta S = \int \frac{\Delta C_p}{T} \mathrm{d}T \tag{4}$$

In Figure 5, the ΔS values in the phase transition temperature range are plotted.

3. Discussion

As regards the urea sublattice, this phase transition is characterized by a change of the space group from $P6_122$ to $P2_12_12_1$. The unit cell volume of the orthorhombic phase (neglecting the effect of the homogeneous strain) becomes twice as large as in the hexagonal phase; i.e., $P2_12_12_1$ is a general subgroup of $P6_122$ of index 6. The reduction of symmetry takes place in two steps: the loss of the 6-fold symmetry leads to the translationengleiche subgroup $C222_1$ of $P6_122$ of index 3. The loss of translations is described by the second step, $C222_1 \rightarrow P2_12_12_1$. There are three $P2_12_12_1$ subgroups of $P6_122$ belonging to one class of conjugate subgroups. The three subgroups are related to the three possible orientational orthorhombic domains within the hexagonal lattice. To every orientational domain corresponds two antiphase domains whose symmetry is described by the same $P2_12_12_1$ subgroup.

In our further discussion, we will consider a representative of the $P2_12_12_1$ conjugate class with the following unit cell vectors ($\vec{a}$, $\vec{b}$, $\vec{c}$) (see Figure 1b):

$$\vec{a} = 2\vec{a}_h + \vec{b}_h$$
$$\vec{b} = \vec{b}_h$$
$$\vec{c} = \vec{c}_h \tag{5}$$

where ($\vec{a}_h$, $\vec{b}_h$, $\vec{c}_h$) are the hexagonal unit cell vectors. The corresponding origin shift of $P2_12_12_1$ with respect to $P6_122$ is given by the origin shift vector $P = (1/2, 1/4, 1/12)$.

In the description of this phase transition mechanism, we have to consider the contribution of the primary and secondary modes to the symmetry—breaking distortion. The phase transition is accompanied by a change of the unit cell volume, which indicates that the symmetry break (the primary modes) can be associated with a Brillouin-zone boundary point. The wave vector describing such a change of the translational symmetry is given by the point M (1/2, 0, 0). The little co-group of M is the point group 222, and all little-group irreducible representations are one-dimensional. Because the star of the wave-vector M is composed of three arms, each little-group irreducible representation induces a three-dimensional M_i, $i = 1,...,4$ irreducible representation of the space group $P6_122$.

Following the notation of Cracknell et al.,[21] the active irreducible representation responsible for the symmetry break $P6_122 \rightarrow P2_12_12_1$ is M_2. In general, the corresponding order parameter is three-dimensional. However, in our specific case, $P2_12_12_1$ is an isotropy subgroup of M_2 with an order parameter direction (q_1, 0, 0). According to the Landau theory, the phase transition $P6_122 \rightarrow P2_12_12_1$ may have a continuous character as the driving order parameter of symmetry M_2 (q_1, 0, 0) satisfies both the Landau and Lifschitz conditions.

Apart from the primary modes, secondary modes may also contribute to the structural distortion of the low-symmetry phase. In the studied case, the secondary modes are related with a Brillouin-zone center representation, which corresponds to the symmetry break $P6_122 \rightarrow C222_1$. The group $C222_1$ is the isotropy group of the two-dimensional irreducible representation Γ_5,[21] with (η_1, 0) as order parameter direction.

The studied phase transition involves a change of the crystal system, so it is also necessary to explore the correlation between the primary order parameter and the structural spontaneous strain (second-order parameter). In this case, the free energy F expansion contains three terms and can be written as

$$F = F_q + F_\epsilon + F_{q\epsilon} \tag{6}$$

$$F_q = \frac{1}{2}\alpha q_1^2 + \frac{1}{4}\beta q_1^4 + \frac{1}{6}\gamma q_1^6 \tag{6a}$$

$$F_\epsilon = \frac{1}{2}\sum_{i,k} C_{ik}^0 \epsilon_i \epsilon_k \tag{6b}$$

$$F_{q\epsilon} = \sum_{i,m,n} \lambda_i \epsilon_i^m q^n \tag{6c}$$

The term F_q is the free energy expansion up to the order six term (eq 6a), in the primary order parameter (where, as usual, only α is considered temperature dependent: $\alpha = A(T_c - T)$, and A, β, and γ are constant values). The second term F_ϵ (eq 6b) is due to the elastic energy, described by the strain tensor components ϵ_i and the elastic constants of the paraelastic phase C_{ik}^0. Finally, the third term (eq 6c) is related to the interaction

energy between the order parameter and the strain. It represents the coupling energy in order n for the order parameter and in order m for the strain. In this case, the breaking shear components ϵ_i and the driving order parameter q_1 have different symmetries (they are associated with different irreducible representations of $P6_122$). The symmetry breaking components of the spontaneous strain $\epsilon_1^S = 0.5(\epsilon_1 - \epsilon_2)$ plays the role of a secondary order parameter. It transforms according to the irreducible representation Γ_5 of $P6_122$. Taking into account the direction of the secondary order parameter for the break $P6_122 \rightarrow C222_1$, the lowest order coupling term allowed by symmetry is linear in the spontaneous strain and quadratic in the order parameter:

$$F_{q\epsilon} \approx \lambda(\epsilon_1 - \epsilon_2)q_1^2 \tag{7}$$

According to the well-accepted classification scheme,[22] the phase transition is described as an improper ferroelastic and belongs to the 622F222 Aizu type. Using the transformation properties of the strain components, one can write down the elastic part of the free energy F_ϵ:

$$F_\epsilon = \frac{1}{2}C_{11}^0(\epsilon_1^2 + \epsilon_2^2) + \frac{1}{2}C_{33}^0\epsilon_3^2 + C_{12}^0\epsilon_1\epsilon_2 + C_{13}^0(\epsilon_1 + \epsilon_2)\epsilon_3 \tag{8}$$

Here, we have taken into account also the non-symmetry breaking terms $(\epsilon_1 + \epsilon_2)$, ϵ_3. The lowest order terms allowed by symmetry are included as we assume the higher orders terms negligibly small.

For determing the correlation between the order parameter q_1 and ϵ_i, the condition

$$\left(\frac{\partial F_{(q,\epsilon)}}{\partial \epsilon_i}\right) = 0 \tag{9}$$

is used. This leads to the following solutions:

$$\epsilon_1 = Kq_1^2 \tag{10a}$$

$$\epsilon_2 = -Kq_1^2 \tag{10b}$$

$$\epsilon_3 = 0 \tag{10c}$$

where

$$K = \frac{2C_{13}^0 2 - C_{11}^0 C_{33}^0 - C_{12}^0 C_{33}^0}{C_{11}^0 2C_{33}^0 + 2C_{12}^0 C_{13}^0 2 - 2C_{11}^0 C_{13}^0 2 - C_{12}^0 2C_{33}^0}\lambda \tag{11}$$

As a result, the scalar spontaneous strain ϵ_A (eq 3) is quadratic in the order parameter

$$\epsilon_A \propto q_1^2 \tag{12}$$

As in eq 6a, only α is temperature dependent; then the excess entropy defined as

$$\Delta S = \left(\frac{\partial F}{\partial T}\right)_{p,q,\epsilon} \tag{13}$$

is also quadratic in the order parameter q_1

$$\Delta S \propto q_1^2 \tag{14}$$

and from eqs 12 and 14, ΔS is linearly related to the scalar spontaneous strain ϵ_A.

$$\Delta S \propto \epsilon_A \tag{15}$$

The dielectric impermeability tensor coefficients ΔB_i, are related with the strain tensor component due to the elasto-optic effect[19]

$$\Delta B_i = p_{ij}\epsilon_j \tag{16}$$

where p_{ij} are the elasto-optical coefficients in the prototype phase.

In the prototype phase, the relation between B_i and the refractive index n is $B_i = (1/n^2)$.[19] Using this relation, one finds that the dependence of ΔB_1 and ΔB_2 on the refractive indices provoked by the 622F222 phase transition are, respectively

$$\Delta B_1 = -\left(\frac{2}{n_h^3}\right)\Delta n_1 \tag{17}$$

$$\Delta B_2 = -\left(\frac{2}{n_h^3}\right)\Delta n_2 \tag{18}$$

where n_h is the ordinary refractive index in the hexagonal parent phase and Δn_1 and Δn_2 are the changes along the x and y directions, respectively. From eqs 16−18, the measured birefringence can be expressed as

$$\Delta n = \Delta n_1 - \Delta n_2 = \frac{1}{2}n_h^3(\epsilon_1 - \epsilon_2)(p_{12} - p_{11}) \tag{19}$$

If p_{12} and p_{11} are not temperature dependent, the spontaneous birefringence is linearly related to the spontaneous strain, and from eq 10, Δn is also quadratic in the order parameter

$$\Delta n \propto q_1^2 \tag{20}$$

Moreover, from eqs 14 and 20, we obtain the expression

$$\Delta S \propto \Delta n \tag{21}$$

As cited above, one of the more interesting features of the C17 low-temperature phase transition is the presence of a double peak in the specific heat curve obtained by adiabatic calorimetry on a powdered sample. This reproducible result also agrees with the AC calorimetric data, where a single crystal was used in the experiments.[14] The first peak with higher C_p values represents the main contribution to the phase transition entropy (ΔS) and takes place at $T_{c1} = 158.8$ K. The second one appears at $T_{c2} = 159.7$ K, and its contribution to ΔS can be estimated at about 15−20% of the total value. The presence of this secondary peak induces a characteristic additional small shoulder in the integrated ΔS curve (see Figure 6). This result can be compared with the experimental spontaneous strain curve, where the same feature can be appreciated. This fact reinforces the intrinsic character of the two-step mechanism driving this phase transition, which cannot be assigned neither to the sample impurities or defects nor to its mono- or polycrystalline character.

The conclusions of the theoretical model developed above lead to simple relations between the excess entropy ΔS and the spontaneous strain ϵ_A and birefringence Δn. A noticeable linear dependence between these experimental quantities and ΔS is observed from 135 up to 158.6 K, 0.2 °C below T_{c1}, showing the validity of eqs 15 and 21 in this temperature range (Figure

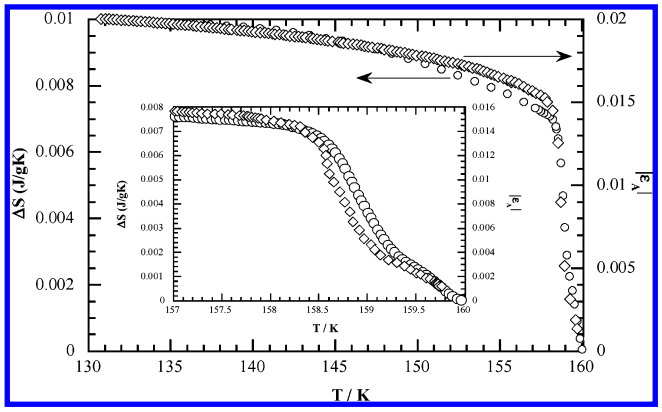

Figure 6. Excess of entropy ΔS (○) and the spontaneous strain of Aizu $|\epsilon_A|$ (◇), showing the correlation between both quantities in agreement with eq 15.

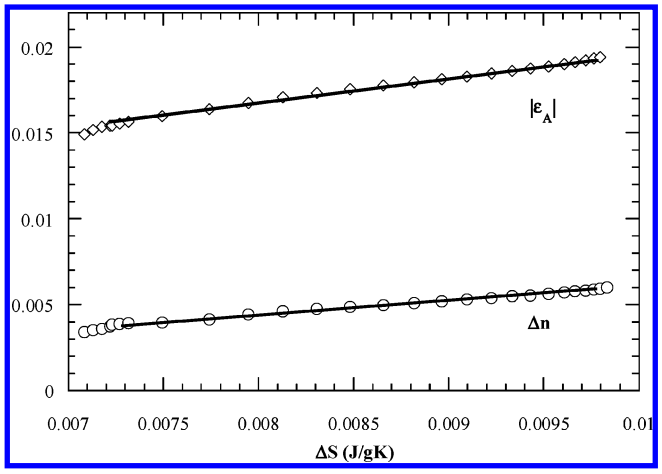

Figure 7. Spontaneous strain of Aizu ϵ_A (◇) and birefringence Δn (○) vs excess of entropy ΔS. In agreement with eqs 15 and 21, a linear relation from 135 to 158.6 K is observed.

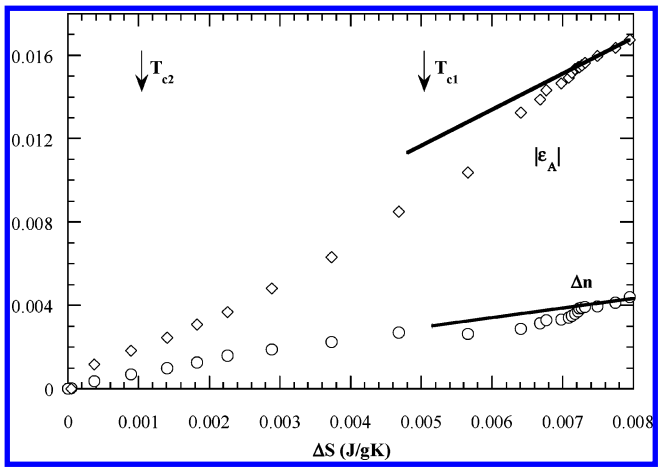

Figure 8. Spontaneous strain of Aizu ϵ_A (◇) and birefringence Δn (○) vs excess of entropy ΔS in the vicinity of the phase transition temperature. The results clearly diverge from the model in this short temperature range (1.7 °C). The arrows show the position of the two specific heat peaks.

7). As usual, these kind of phenomenological models do not properly describe the physical quantities near the transition temperature due to critical phenomena associated to the order parameter. In our case, the validity of eqs 15 and 21 above 158.6 K is even worse due to the secondary anomaly at T_{c2}. The discrepancies can be seen in Figure 8, which emphasizes the lack of linearity in the ϵ_A and Δn vs ΔS plot near T_{c1} and T_{c2}. These results as well as the form of the specific heat curves

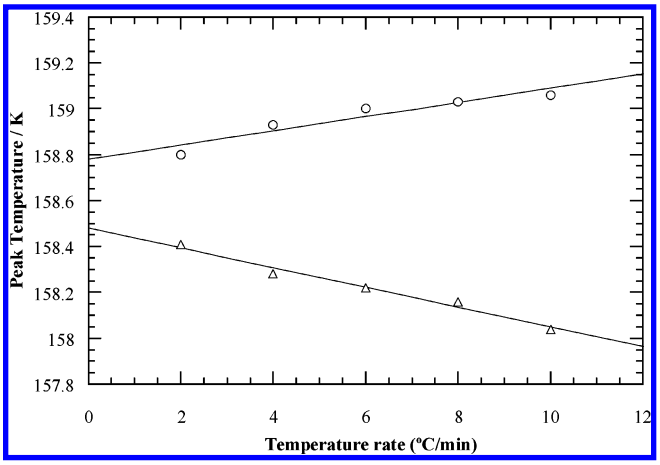

Figure 9. Peak temperature vs temperature rate in C17 from DSC measurements: (○) heating runs, (△) cooling runs. Linear extrapolations to zero-rate give a thermal hysteresis of 0.30 °C.

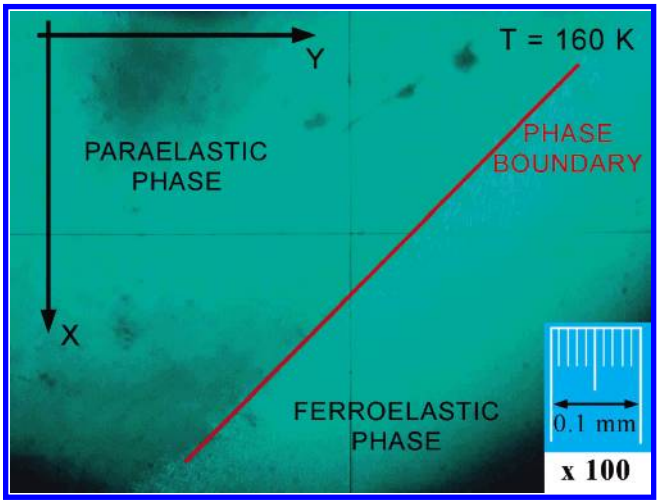

Figure 10. Phase boundary between the hexagonal−orthorhombic phases at 160 K in C17 crystal.

(Figure 4) indicate the first-order character of the observed phase transitions. These features are confirmed by the (small) thermal hysteresis of 0.30 °C for the main peak detected by the DSC calorimetric measurements (Figure 9).

The first-order character of the transformation becomes also obvious from the distribution of the phase boundaries between the hexagonal−orthorhombic phases found at the transition temperature (Figure 10). The phase boundary has almost the shape of a straight line with an angle of 45° with the *x*-axis. This direction agrees with the extended theory of Sapriel for 622F222 ferroelastic phase transition.[16] In contrast, similar experiments in C19[23] show neither thermal hysteresis nor evidence of any phase boundaries at the transition temperature. An additional argument that supports the first-order character of this phase transition comes from the negative value of the β coefficient (eq 6a) determined from the ΔS evolution as a function of the temperature (Figure 5).

The linear behavior of spontaneous strain ϵ_A and birefringence Δn is limited to the 0.007 J/gK < ΔS < 0.010 J/gK range, which corresponds to 158.6 > T > 135 K. Near both peaks, the experimental behavior is, however, different from the theoretical predictions. It should be stressed that this model is limited to describe the $P6_122 \rightarrow P2_12_12_1$ transformation of the urea sublattice, omitting any influence of the alkane chains in the phase transition mechanisms. The ordering of these chains in the urea tunnels seems to start at higher temperatures above

T_{c1} and is referred to pretransitional effects, observed in C19 by NMR and neutron measurements.[10] The ordering and freezing of the guest molecules' rotational motion around the channels' axes corresponds to an increase of the lateral orientational correlation, but the longitudinal ordering process is unaffected by the phase transition.[8] These orientational processes are expected to be more relevant as the phase transition temperature is approached, where the rearrangements of the urea channels (T_{c2}) finally make the alkane ordering (T_{c1}) easier. If this effect is responsible for the observed C_p secondary peak or not, it cannot be established from the available experimental information. It should be noted that the C19 crystal also shows this double anomaly, but it is not present in the deuterated derivative.[23] In the latter case, the presence of only one peak could be related to the weaker interaction between the host and guest substructures due to the hydrogen−deuterium substitution, which favors the coupling of the corresponding transition processes. The influence of the alkane molecules in the phase transition mechanism seems to be out of question and can explain the failure of theoretical models only based on the urea transformation. A more adequate model should take into account the interaction between the guest and the host subsystem to incorporate the dynamics of the *n*-alkane molecules in the construction of the free energy expansion to avoid discrepancies (especially visible near the temperature of the phase transition) between the experimental results and the proposed theoretical model. Different from the above-discussed model of the observed transformations is the model supposing an intermediate phase of symmetry $C222_1$ between the two-end phases ($P6_122 \rightarrow P2_12_12_1$). However, a structural study around this temperature range is required for a better understanding of the observed two-step transition mechanism. Following previous experiments performed in C19,[24,25] a similar work on C17 is now in progress. It is focused on the thermal behavior of the superstructure line intensities along the incommensurate crystallographic c^* direction.

Acknowledgment. Authors acknowledge financial support from the University of the Basque Country (projects UPV 13646/2004 and UPV 13562/2001) and the Ministry of Science and Technology (project MAT2004-03166), as well as from the Basque Government in the frame of the Strategic Plan for Science and Technology (ETORTEK-ACTIMAT-2005).

References and Notes

(1) Takemoto, K.; Sonoda, N. *Inclusion Compounds*; Academic Press: London, 1984.
(2) Smith, A. E. *Acta Crystallogr.* **1952**, *5*, 224.
(3) George, A. R.; Harris, K. D. M. *J. Mol. Graphics* **1995**, 13, 138.
(4) van Smaalen, S.; Harris, K. D. M. *Proc. R. Soc. London* **1996**, *452*, 677.
(5) Fukao, K.; Miyaji, H.; Asai, K. *J. Chem. Phys.* **1986**, *84*, 6360.
(6) Schlenk, W. *Liebigs Ann. Chem.* **1949**, *565*, 204.
(7) Forst, R.; Jagodzinski, H.; Boysen, H.; Frey, F. *Acta Crystallogr.* **1987**, *B43*,187−197.
(8) Weber, T.; Boysen, H.; Frey, F. *Acta Crystallogr.* **2000**, *B56*, 132−141.
(9) Boysen, H. *Phase Transitions* **1995**, *55*, 1.
(10) Le Lann, H.; Odin, C.; Toudic, B.; Ameline, J. C.; Gallier, J.; Guillaume, F.; Breczewski, T. *Phys. Rev. B* **2000**, *62* (9), 5442−5451.
(11) Lynden-Bell, R. M. *Mol. Phys.* **1993**, *79*, 313.
(12) Rubio-Peña, L.; Breczewski, T.; Bocanegra, E. H. *Ferroelectrics* **2002**, *269*, 171−176.
(13) Rubio Peña, L. Ph.D. Thesis. Universisdad del País Vasco, 2003
(14) Fraile-Rodriquez, A.; Ruiz-Larrea, I.; Rubio-Peña, L.; López-Echarri, A. *Eur. Phys. J.* **2001**, *B24*, 189−195.
(15) Salje, E. K. M. *Phase Transitions in Ferroelastic and Co-Elastic Crystals*; Cambridge University Press: Cambridge, U.K., 1990.
(16) Sapriel J. *Phys. Rev.* **1975**, *B12*, 5128.
(17) Menard, K. P. *Dynamic mechanical analysis: a practical introduction*; CRC Press LLC: Boca Raton, FL, 1999.
(18) Carpenter, M. A.; Salje, E. K. H.; Graeme-Barber, A. *Eur. J. Mineral.* **1998**, *10*, 621−691.
(19) Nye, J. F. Physical properties of crystals; Oxford University Press: Oxford, U.K., 1985.
(20) Aizu, K. *J. Phys. Jpn.* **1970**, *28* (3), 706.
(21) Cracknell, A. P.; Davies, B. L.; Miller, S. C.; Love, W. F. Kroneker product tables; *General introduction and tables of irreducible representation of space groups*; Plenum: New York, 1979; Vol. 1.
(22) Wadhawan, V. K. *Phase Transitions* **1982**, *3*, 3−103.
(23) López-Echarri, A.; Ruiz-Larrea, I.; Fraile-Rodriquez, A.; Díaz-Hernández, J.; Breczewski, T.; Bocanegra, E. H. To be published.
(24) Toudic, B.; Aubert, F.; Ecolivet, C.; Bourges, P.; Breczewski, T. *Phys. Rev. Lett.* **2006**, *96*, 145503.
(25) Toudic, B.; Garcia, P.; Odin, C.; Rabiller, P.; Ecolivet, C.; Bourges, P.; Breczewski, T. To be published.